Plant Science Horizons

Research Article

Open-Access

Plant Science Horizons 2026, 1(2): e0013
https://doi.org/10.66835/psh.2026.e0013

Check for updates

Genome-Wide Identification and Expression Profiling of the Laccase Gene Family in Tomato (*Solanum lycopersicum*) under Abiotic Stress and Hormonal Treatments

Sidra Ashraf[1], Farwa Yaqoob[1], Noor ul Ain[1], Sana Basharat[2]*

[1]*Department of Biochemistry, University of Agriculture Faisalabad, Pakistan*
[2]*School of Breeding and Multiplication (Sanya Institute of Breeding and Multiplication), School of Tropical Agriculture and Forestry, Hainan University, Sanya 572025, China*
***Correspondence:** sanabasharat143@gamail.com (Basharat S)

Abstract

Laccases (LACs) are multicopper oxidases involved in lignin polymerization, cell wall development, and plant responses to environmental stimuli. This study identified 24 candidate SlLAC genes in the tomato genome and characterized their protein properties, chromosomal distribution, gene structures, conserved sequence regions, phylogenetic relationships, predicted subcellular localization, and potential miR397 targeting. The predicted proteins ranged from 484 to 614 amino acids and from 53.78 to 68.72 kDa. Most had basic theoretical isoelectric points, and all had negative GRAVY values. The genes occurred on 10 of the 12 tomato chromosomes; chromosome 5 contained five members, while chromosomes 6 and 9 each contained four. Conserved laccase-associated sequence regions supported their classification as candidate multicopper oxidases. The reported expression profiles varied among tissues, fruit developmental stages, and salt, drought, cold, and hormonal treatments. *SlLAC23* showed elevated reported values in several vegetative and young-fruit samples, whereas *SlLAC22* showed a pronounced flower-associated profile. Eight genes were predicted as potential sly-miR397 targets. These computational predictions and descriptive expression patterns identify candidates for subsequent functional studies; they do not establish enzyme activity, subcellular localization, miRNA-mediated regulation, or stress-tolerance functions experimentally.

Keywords: *Solanum*; multicopper oxidase; lignification; gene family; expression profiling; miR397

Citation: Ashraf, S., Yaqoob, F., Ain, N. U., & Basharat, S. (2026). Genome-Wide Identification and Expression Profiling of the Laccase Gene Family in Tomato (*Solanum lycopersicum*) under Abiotic Stress and Hormonal Treatments. Plant Science Horizons 1(2): e0013 https://doi.org/10.66835/psh.2026.e0013

Introduction

Laccases (LACs; EC 1.10.3.2) are multicopper oxidases that oxidize suitable substrates while reducing molecular oxygen to water [1, 2]. Oxygen acts as the terminal electron acceptor, rather than an electron donor. Plant laccases contribute to lignin polymerization and cell wall development. Lignin

© The Author(s)

provides mechanical support and contributes to vascular function. Functional studies in *Arabidopsis thaliana* have demonstrated roles for *LAC4* and *LAC17* in stem lignification and have established that laccases are not functionally interchangeable with peroxidases during vascular development [3, 4]. Other members, including TRANSPARENT TESTA10, participate in oxidative polymerization of seed-coat flavonoids [5].

Genome-wide LAC-family studies in *Arabidopsis*, rice, soybean, tea, rapeseed, common bean, and citrus have identified variation in family size, gene structure, and expression patterns [6, 7, 8, 9, 10, 11, 12, 13]. Such comparative studies provide hypotheses about evolutionary and regulatory diversification, but family size or physical proximity alone does not demonstrate duplication in a particular lineage. Post-transcriptional regulation is another relevant layer: miR397-mediated regulation of laccases has been experimentally investigated in poplar and *Arabidopsis*, including effects on lignin accumulation and root lignification under resource limitation [14, 15, 16].

Tomato (*Solanum lycopersicum*) is an important horticultural crop and a model for studying fruit development and plant environmental responses [17]. Characterizing its candidate LAC genes can help prioritize targets for functional analysis. Computational annotation, predicted miRNA interactions, and expression associations should nevertheless be distinguished from demonstrated molecular functions.

This study aimed to identify candidate tomato LAC genes and describe their physicochemical properties, genomic distribution, exon–intron structures, conserved sequence regions, phylogenetic relationships, predicted localization, potential miR397 targeting, and reported expression profiles across tissues, fruit stages, abiotic stresses, and hormonal treatments. The analysis was intended to identify candidates and hypotheses for subsequent experimental validation, rather than to establish causal roles in lignification, fruit ripening, or stress tolerance.

Materials and Methods

Identification of *SlLAC* genes

Tomato genome sequence and annotation files were obtained from the Sol Genomics Network (https://solgenomics.net/feature/19730682/details). *Arabidopsis* LAC protein sequences obtained from TAIR (https://www.arabidopsis.org/) were used as queries for BLASTP searches of the tomato protein database, using an E-value cutoff of ≤ 1×10^{-5}. Hidden Markov model profiles associated with multicopper oxidases were also searched against the tomato proteome using HMMER [18]. The relevant Pfam accessions are PF00394, PF07731, and PF07732; PF007731 in the original text was an accession typographical error. Candidate sequences were examined for conserved domains using SMART and NCBI CDD [19, 20].

Amino acid length, molecular weight, theoretical isoelectric point, and grand average of hydropathy (GRAVY) were calculated using ExPASy ProtParam [21]. Chromosome identifiers and genomic coordinates were taken from the annotation file and visualized with TBtools [22]. Subcellular localization was predicted using WoLF PSORT [23]. Coding and genomic sequences were compared using GSDS to display exon–intron organization [24]. Localization assignments are predictions, not experimental observations. No synteny, duplication classification, or Ka/Ks analysis is presented here; therefore, chromosome proximity is not used as evidence of duplication or family expansion.

Multiple sequence alignment and phylogeny of LAC gene family

Candidate LAC protein sequences were aligned using ClustalW in MEGA7 [25, 26], and conserved sequence regions were displayed with ESPript [27].

Unrooted neighbor-joining trees were constructed with the Poisson amino acid substitution model and 1,000 bootstrap replicates. Separate trees were prepared for the tomato proteins and for the combined tomato–*Arabidopsis* protein set. Bootstrap percentages represent the proportion of resampled alignments supporting a node. The supplied trees are exploratory; weakly supported deeper relationships are not treated as resolved evolutionary histories. A maximum-likelihood robustness analysis is not presented, and no such analysis is claimed to have been performed.

miRNA target prediction analysis

Potential sly-miR397 target sites in SlLAC coding sequences were predicted using psRNATarget [28]. The original analysis was described as using default settings. Expectation scores and unpaired energy (UPE) values were retained as computational outputs. The expectation score summarizes complementarity under the server scoring scheme; UPE estimates the energetic cost of opening the target region for small-RNA access. Lower values can indicate more favorable predicted matching or accessibility, respectively, but neither measure establishes in vivo cleavage, binding affinity, or regulatory strength.

Plant Material and Growth Conditions

Surface-sterilized seeds of the tomato cultivar Micro-Tom were grown in a greenhouse with a 14 h light/10 h dark photoperiod, day/night temperatures of 25/20 °C, and 60% relative humidity. Plants were irrigated with nutrient solution once per week. Roots, stems, and leaves were collected from two-month-old plants. Flower buds, open flowers, and fruits at immature, breaker, and red stages were collected at the corresponding developmental stages. Samples were harvested between 9:00 and 10:00 a.m. and immediately frozen in liquid nitrogen. The original protocol reports sampling from six healthy plants and three independent biological replicates; the pooling arrangement and correspondence of these samples to the expression datasets require confirmation from the experimental records.

Hormone and Abiotic Stress Treatments

For hormonal treatments, 12-day-old tomato seedlings were immersed in liquid Murashige and Skoog (MS) medium supplemented with 20 μM ethephon (Eth), gibberellic acid (GA_3), indole-3-acetic acid (IAA), salicylic acid (SA), or jasmonic acid (JA). Seedlings maintained in hormone-free MS medium served as controls. Root and shoot samples were collected separately at 0, 3, 6, 9, and 12 h after the initiation of each treatment to investigate time-dependent gene expression responses. All collected samples were immediately frozen in liquid nitrogen and stored at −80 °C until further analysis.

One-month-old plants were subjected to abiotic stress treatments, including cold stress at 4 ± 1 °C and salt stress with 200 mM NaCl. Leaf samples were collected at 0, 3, 6, 9, and 12 h after the initiation of each treatment to assess time-dependent responses. For drought stress, water was withheld from the plants for up to 15 days, while control plants were maintained under well-watered conditions. At each sampling time point, leaf tissues from six independent plants were pooled to constitute one biological replicate, and three independent biological replicates were collected per treatment. All harvested samples were immediately frozen in liquid nitrogen and stored at −80 °C until further analysis.

RNA Isolation and Real-Time Quantitative PCR Analysis

Total RNA was extracted using TRIzol reagent (Invitrogen, USA). RNA quality was assessed by 1.2% agarose gel electrophoresis and a NanoDrop 1000 spectrophotometer (Thermo, USA). First-strand cDNA was synthesized from 2 μg total RNA using the PrimeScript RT Reagent Kit with gDNA Eraser (TaKaRa,

Japan). RT-qPCR was performed with SsoAdvanced Universal SYBR Green Supermix (Bio-Rad, USA) on a CFX96 Touch Real-Time PCR Detection System. Each 20 µL reaction contained 10 µL master mix, 1 µL cDNA, 0.5 µL of each primer, and 8 µL nuclease-free water. The reported cycling program was 95 °C for 30 s, followed by 40 cycles of 95 °C for 5 s and 58 °C for 20 s. Melting curves were collected over 60–95 °C to assess amplification specificity. The original protocol states that relative expression was calculated by the $2^{-}\Delta\Delta Ct$ method with *SlUBI* as the reference gene [29].

Results

Identification and physicochemical characterization of *SlLAC* genes

The reported analysis retained 24 candidate tomato LAC genes, listed in Table 1. Their predicted proteins ranged from 484 amino acids for SlLAC2 to 614 amino acids for SlLAC14, with molecular weights of 53.78–68.72 kDa (Table 1). The theoretical isoelectric points ranged from 6.51 for SlLAC6 to 10.21 for SlLAC19. Most values were above 7, indicating predominantly basic predicted proteins. These parameters describe sequence-derived properties and do not establish catalytic activity or the intracellular environment in which a protein functions.

All predicted proteins had negative GRAVY values, ranging from −0.330 to −0.001. SlLAC1 and SlLAC5 had values of −0.330 and −0.315, respectively, whereas SlLAC22 was close to neutral at −0.001. Negative values indicate an overall hydrophilic sequence tendency, rather than evidence of cytosolic localization or a particular biochemical role. Table 1 places 13 genes on the positive strand and 11 on the negative strand. Strand orientation alone does not establish transcriptional regulatory changes, genome rearrangements, or evolutionary mechanisms.

WoLF PSORT predicted chloroplast localization for 14 of the 24 proteins: SlLAC7–10, SlLAC12–17, SlLAC19, and SlLAC21–23. Other predicted assignments were extracellular for SlLAC1, SlLAC3, SlLAC11, and SlLAC18; peroxisomal for SlLAC6 and SlLAC20; and mitochondrial, vacuolar, endoplasmic-reticulum, or cytoplasmic for the remaining members (Table 1). These assignments are provisional. The frequent chloroplast predictions differ from the well-established extracellular and cell-wall roles of many plant laccases and require assessment of secretion signals, transit peptides, and experimental localization before biological interpretation.

Table 1 summarizes locus identifiers, protein length, molecular weight, theoretical pI, GRAVY, chromosome coordinates, strand orientation, exon number, and predicted subcellular localization. Sequence-derived similarities and differences identify candidates for further investigation; they do not demonstrate functional differentiation.

Chromosomal Distribution of *SlLAC* Genes

The 24 genes occurred on 10 of the 12 tomato chromosomes: chromosomes 1, 2, 4, 5, 6, 7, 9, 10, 11, and 12. Chromosome 5 contained five genes; chromosomes 6 and 9 each contained four; chromosome 2 contained three; chromosomes 4 and 10 each contained two; and chromosomes 1, 7, 11, and 12 each contained one (Table 1; Figure 1). No identified member was assigned to chromosome 3 or 8. This is a marked uneven distribution, but no statistical test of chromosome enrichment is reported. Closely positioned genes can motivate duplication analyses, although physical proximity alone does not demonstrate a duplication event.

Results

Gene Structure Analysis

The reported SlLAC gene models contained 4–7 exons, with most containing six (Table 1; Figure 2). *SlLAC2* contained four exons, whereas *SlLAC7* and *SlLAC12* contained seven. Differences in exon–intron organization document structural variation among the gene models. They may reflect evolutionary changes,

but this analysis does not establish the direction of intron gain or loss, selection pressure, or functional consequences.

Multiple Sequence Alignment and Phylogeny of SlLAC Proteins

Alignment of the 24 predicted SlLAC proteins showed conserved laccase-associated sequence regions designated L1–L4 (Figure 3) [31]. Histidine- and cysteine-containing residues within these regions are consistent with the copper-binding architecture of multicopper oxidases. The displayed L1 region contains an HWHG-related sequence in many members, although substitutions are visible in some proteins. Conservation supports classification as candidate laccase-like proteins; it does not demonstrate copper occupancy, metal-binding affinity, or enzyme activity.

The L2 and L3 regions contain conserved histidine-rich positions, consistent with laccase-associated copper-binding sequence signatures. Amino acid substitutions occur at some positions, while other residues are shared across the family (Figure 3). The alignment is descriptive and does not provide a test of selection pressure or demonstrate differences in catalytic efficiency.

The L4 region includes conserved histidine- and cysteine-containing sequences, with variation among individual members (Figure 3). These sequence features support the annotation of candidate multicopper oxidases. Proposed differences in substrate preference or catalytic properties require biochemical validation and are not inferred from the alignment alone.

The tomato-only neighbor-joining tree displays labels G1–G5, with G4 subdivided into G4_A and G4_B (Figure 4, left), giving six labeled terminal categories rather than seven independent principal groups. The supplied tree places SlLAC2, SlLAC3, SlLAC4, SlLAC15, and SlLAC20–22 in G2; SlLAC14, SlLAC17, SlLAC18, and SlLAC19 in G1; SlLAC9–13 in G3; SlLAC7 and SlLAC16 in G5; SlLAC6 and SlLAC24 in G4_A; and

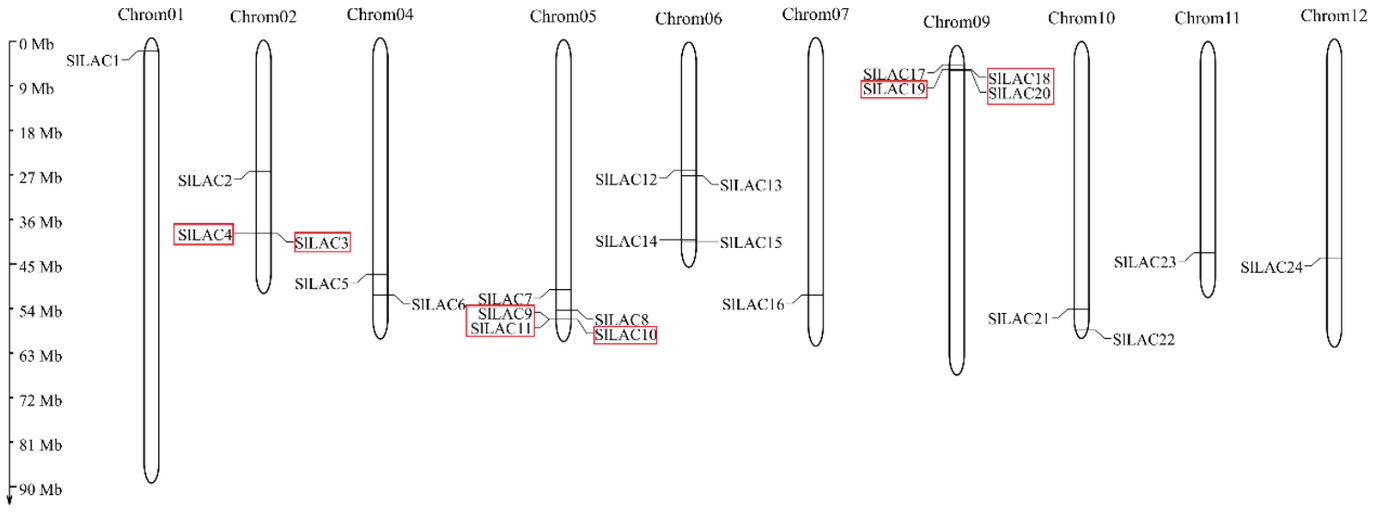


Figure 1. Chromosomal distribution of the 24 candidate SlLAC genes on 10 of the 12 tomato chromosomes. Chromosomes 3 and 8 contain no identified member and are not shown. Genomic positions are displayed in megabases (Mb); gene identifiers correspond to Table 1.

Table 1. Sequence-derived properties and genomic information of the 24 candidate SlLAC genes.

Gene ID	Name	aa	MW	pI	GRAVY	Chromosome			Strand	Exon number	Subcellular location prediction
						Number	Start	End			
Solyc01g008830	*SlLAC1*	572	65.05	9.15	-0.33	1	2854277	2862504	+	6	extr
Solyc02g062650	*SlLAC2*	484	53.78	7.79	-0.201	2	28968216	28970551	-	4	mito
Solyc02g085110	*SlLAC3*	559	62.05	8.16	-0.1	2	42674495	42676816	-	6	extr
Solyc02g085120	*SlLAC4*	559	61.82	8.11	-0.069	2	42679480	42681934	-	6	vacu
Solyc04g054690	*SlLAC5*	578	65.51	8.07	-0.315	4	52198899	52201343	-	5	E.R.
Solyc04g072280	*SlLAC6*	567	63.05	6.51	-0.215	4	56905173	56909198	+	6	pero
Solyc05g043360	*SlLAC7*	571	62.96	9.39	-0.092	5	55217891	55222581	+	7	chlo
Solyc05g050540	*SlLAC8*	577	64.58	8.42	-0.155	5	59817624	59820559	-	6	chlo
Solyc05g052340	*SlLAC9*	574	63.37	9.03	-0.176	5	61741956	61744207	-	6	chlo
Solyc05g052390	*SlLAC10*	570	63.12	7.88	-0.119	5	61764704	61767262	+	6	chlo
Solyc05g052400	*SlLAC11*	574	63.38	8.39	-0.158	5	61768562	61770938	+	6	extr
Solyc06g048860	*SlLAC12*	573	63.26	7.58	-0.052	6	28322138	28325214	+	7	chlo
Solyc06g050530	*SlLAC13*	567	61.93	7.29	-0.076	6	29719506	29721992	-	6	chlo
Solyc06g076330	*SlLAC14*	614	68.72	9.66	-0.038	6	43809673	43812715	-	6	chlo
Solyc06g076760	*SlLAC15*	560	62.53	9.09	-0.068	6	44056679	44059629	+	6	chlo
Solyc07g049460	*SlLAC16*	572	63.31	9.06	-0.079	7	57063539	57067729	+	6	chlo
Solyc09g010990	*SlLAC17*	571	63.53	9.57	-0.102	9	4344657	4347241	+	6	chlo
Solyc09g011960	*SlLAC18*	569	63.64	9.16	-0.141	9	5237938	5240382	+	6	extr
Solyc09g011970	*SlLAC19*	579	64.73	10.21	-0.125	9	5244850	5248906	+	6	chlo
Solyc09g014240	*SlLAC20*	561	61.56	9.47	-0.053	9	5730476	5734045	+	6	pero
Solyc10g076830	*SlLAC21*	556	61.1	9.72	-0.056	10	59123721	59126117	-	6	chlo
Solyc10g085090	*SlLAC22*	557	61.41	9.53	-0.001	10	63726967	63730319	+	6	chlo
Solyc11g062440	*SlLAC23*	573	64.22	9.35	-0.303	11	46585315	46591410	-	5	chlo
Solyc12g056820	*SlLAC24*	567	64.36	9.49	-0.302	12	48257800	48261484	-	6	cyto

aa, amino acids; MW, molecular weight (kDa); pI, theoretical isoelectric point; GRAVY, grand average of hydropathy; extr, extracellular; mito, mitochondrion; cyto, cytoplasm; chlo, chloroplast; vacu, vacuole; E.R., endoplasmic reticulum; pero, peroxisome. Localization labels are computational predictions.

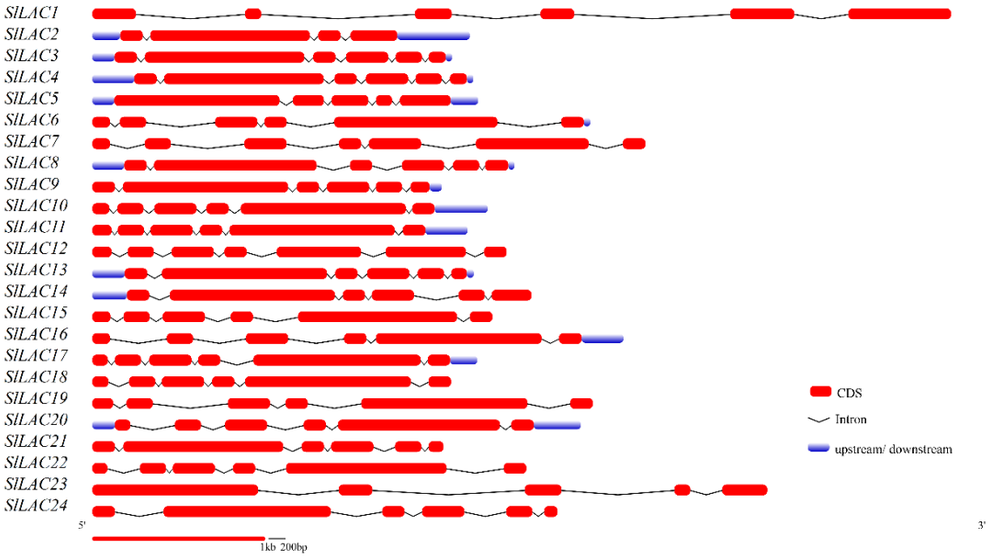


Figure 2. Exon–intron organization of the candidate SlLAC genes in tomato. The diagram compares the reported genomic structures; exon counts are listed in Table 1.

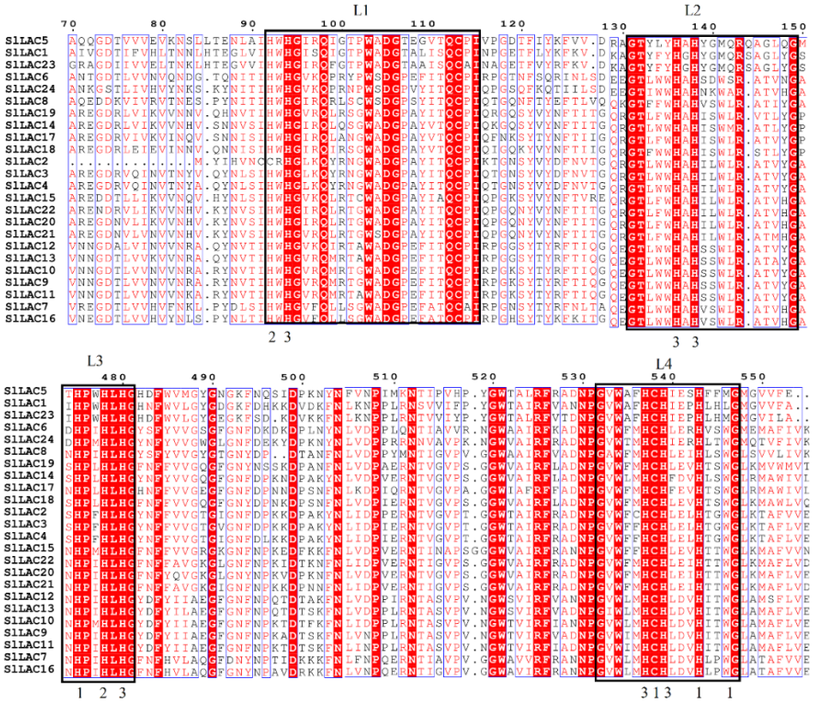


Figure 3. Alignment of conserved L1–L4 sequence regions in the predicted tomato laccases. Highlighted positions indicate sequence conservation. The numbers 1, 2, and 3 beneath selected residues denote proposed associations with type-1, type-2, and type-3 copper sites, respectively; they are not measurements of copper binding in this study.

SlLAC5, SlLAC1, and SlLAC23 in G4_B. SlLAC8 lies on a separate branch whose association with a labeled category is not unambiguously indicated by the supplied group bars. This assignment requires clarification from the tree file.

In the combined tomato–*Arabidopsis* tree (Figure 4, right), the labels are G1–G6. G2 contains SlLAC2–4, SlLAC15, and SlLAC20–22; G1 contains SlLAC14 and SlLAC17–19; G3 contains SlLAC9–13; G5 contains SlLAC7 and SlLAC16; and the broader G4 contains SlLAC1, SlLAC5, SlLAC6, SlLAC8, SlLAC23, and SlLAC24. G6 contains AtLAC1 and no tomato member. The group labels are descriptive conventions for each tree, not evidence that an individual gene has changed biological identity. Several local nodes have bootstrap support of 100%, but deeper relationships include support values of 43% and 66% in the tomato-only tree and 27% and 49% in the combined tree. These weakly supported relationships should be interpreted cautiously. The trees indicate sequence relatedness, rather than experimentally demonstrated functional equivalence.

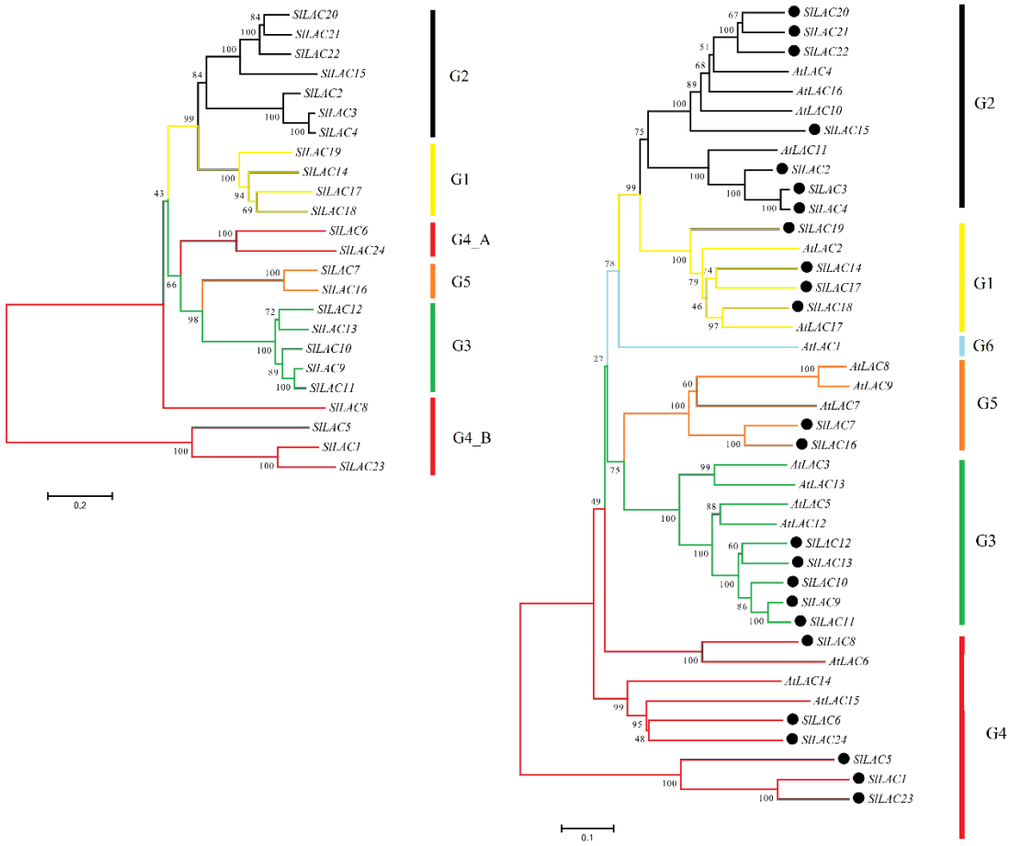


Figure 4. Neighbor-joining phylogenies of candidate laccase proteins. The left panel contains the 24 tomato proteins; the right panel contains the tomato proteins together with *Arabidopsis* homologs. Both trees were generated using MEGA7, the Poisson amino acid substitution model, and 1,000 bootstrap replicates. Node labels indicate bootstrap percentages; scale bars indicate substitutions per site. G1–G5, with G4_A/G4_B subdivisions, are tree-specific labels in the tomato-only panel; G1–G6 are labels in the combined panel. Weakly supported nodes are not interpreted as resolved relationships.

SlLAC Gene Family miRNA Target Prediction Analysis

psRNATarget identified eight SlLAC coding sequences as potential sly-miR397 targets: *SlLAC2*, *SlLAC7*,

SlLAC12, *SlLAC14*, *SlLAC15*, *SlLAC16*, *SlLAC20*, and *SlLAC21* (Table 2). Expectation scores ranged from 0.5 to 2.0, with *SlLAC16* having the lowest score. UPE values ranged from 7.921 to 17.780, with *SlLAC7* having the lowest value. These outputs describe predicted complementarity and accessibility. They do not rank measured binding affinity or establish cleavage, transcript repression, or regulation during stress. miR397 expression and target cleavage were not measured in the reported analysis.

Table 2. Predicted sly-miR397 targets among the SlLAC coding sequences. UPE, unpaired energy, estimates the energetic cost of opening the target site; the expectation score summarizes complementarity under the psRNATarget scoring scheme. Both are prediction outputs and not measurements of regulatory strength.

SGN locus ID	Gene name	Predicted targeting miRNA	miRNA length	UPE	Expectation score
Solyc02g062650	*SlLAC2*	sly-miR397	20	17.78	1.5
Solyc05g043360	*SlLAC7*	sly-miR397	20	7.921	1
Solyc06g048860	*SlLAC12*	sly-miR397	20	13.175	2
Solyc06g076330	*SlLAC14*	sly-miR397	20	14.659	1.5
Solyc06g076760	*SlLAC15*	sly-miR397	20	15.83	2
Solyc07g049460	*SlLAC16*	sly-miR397	20	12.382	0.5
Solyc09g014240	*SlLAC20*	sly-miR397	20	15.811	2
Solyc10g076830	*SlLAC21*	sly-miR397	20	15.639	1

Expression Analysis of *SlLAC* Genes in Different Tissues and Fruit Development Stages

The tissue and fruit-stage heatmap shows variation in the reported expression values for the 24 SlLAC genes (Figure 5). The dataset source, measurement unit, normalization, and color transformation must be established before quantitative interpretation. These profiles are described as associations rather than evidence of tissue-specific biological functions.

In the root column of Figure 5, *SlLAC23* has a reported value of 86.39, whereas *SlLAC16* has 42.45; therefore, *SlLAC16* cannot be described as having the highest displayed value. Other displayed root values include *SlLAC20* (41.49), *SlLAC5* (33.67), *SlLAC4* (18.97), and *SlLAC21* (16.22). Several genes show relatively elevated root-associated values within their own profiles. Without a verified normalization scheme, these numbers should not be interpreted as directly comparable absolute expression across genes or as evidence of root lignification.

SlLAC23 shows a reported leaf value of 31.04, while *SlLAC1* and *SlLAC4* show values of 10.19 and 4.84, respectively (Figure 5). The profiles identify candidates for further study, but do not establish roles in leaf cell wall construction, redox regulation, or maturation.

SlLAC22 shows a pronounced flower-associated profile, with reported values of 1137.02 in flowers and 895.70 in flower buds (Figure 5). These numbers require confirmation of their unit, normalization, and plotting transformation. The profile supports prioritizing this gene for reproductive-tissue studies, but does not demonstrate a role in organ formation or pollen development.

SlLAC23 shows reported values of 70.06, 57.51, and 27.19 in the 1, 2, and 3 cm fruit samples, respectively. *SlLAC5* has a reported mature-green value of 13.43

(Figure 5). These associations suggest developmental variation in expression; effects on cell expansion, ripening, or cell wall remodeling remain hypotheses.

SlLAC10 has a reported breaker-stage value of 1.30, compared with lower displayed values at the earlier fruit stages (Figure 5). Several genes show lower values at the breaker + 10 day stage than in younger fruits. These observations are descriptive and do not establish statistical induction, repression, or a causal role in fruit color change.

Together, the tissue profiles identify genes for developmental follow-up. Their biological significance requires confirmation of the dataset provenance and normalization, followed by replicate-based analysis and functional experiments.

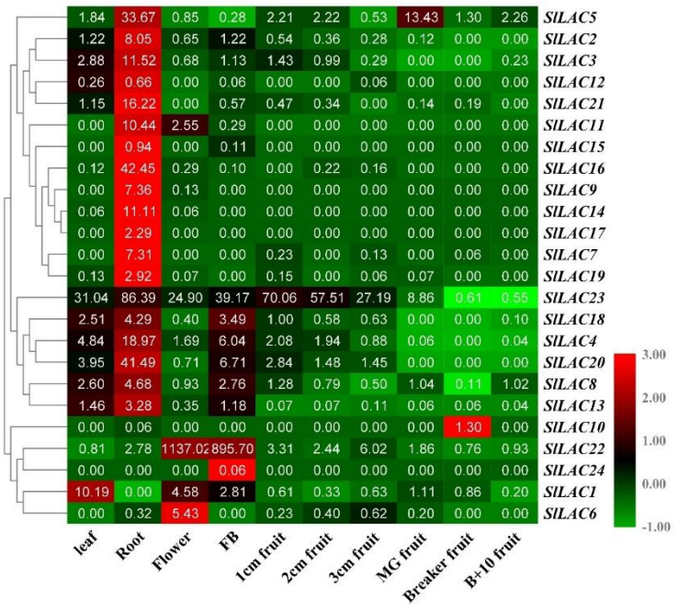


Figure 5. Reported SlLAC expression profiles across tissues and fruit stages. Leaf, root, and flower denote the indicated organs; FB, flower bud; 1–3 cm fruit, young fruit grouped by size; MG, mature green; breaker, onset of visible color change; B+10, 10 days after the breaker stage. Cell annotations retain the originally reported values. Their unit and normalization, and the transformation represented by the color scale, require confirmation; colors are not significance indicators.

Expression Pattern Analysis of *SlLAC* Genes under Salt, Drought, and Cold Stress

Figure 6 presents reported time-course profiles labeled as salt, drought, and cold stress in the Results. The displayed columns are 0, 3, 6, 9, and 12 h. Because these times do not match the supplied experimental protocol, treatment identities, panel order, sampling times, and dataset provenance require verification. Patterns are described without claims of statistically significant regulation or demonstrated stress-tolerance functions.

In the reported salt series, *SlLAC22*, *SlLAC10*, *SlLAC11*, and *SlLAC3* show relatively high plotted values during some early treatment intervals, whereas *SlLAC17*, *SlLAC13*, and *SlLAC19* show higher values at later displayed intervals. *SlLAC7*, *SlLAC2*, and *SlLAC9* generally show lower plotted values (Figure 6). These visual patterns alone do not establish differential expression, treatment insensitivity, or a role in ROS scavenging.

The series labeled as drought shows relatively high plotted values for *SlLAC1*, *SlLAC3*, *SlLAC10*, and *SlLAC15* at later displayed intervals, and for *SlLAC21* and *SlLAC22* at an early interval (Figure 6). The hourly labels must be reconciled with the water-withholding protocol described in Methods. The heatmap does not demonstrate water-retention mechanisms, antioxidant activity, or stress tolerance.

In the series labeled as cold stress, the plotted profiles of *SlLAC14*, *SlLAC10*, *SlLAC1*, *SlLAC23*, and *SlLAC8* differ over the early displayed intervals. *SlLAC17* shows a higher value at 9 h, while *SlLAC5* and *SlLAC6* show higher values at 12 h in the reported interpretation. Cold stress, rather than cryogenic treatment, is the appropriate term for the described 4 °C treatment. Lower plotted values for *SlLAC20* do not establish that the gene lacks a cold-response function.

The displayed dendrograms group genes by the reported expression profiles. Similar clustering patterns are exploratory associations and do not demonstrate shared regulatory pathways or functional equivalence. The clustering distance, linkage method, and any row scaling must be documented.

The reported stress profiles nominate candidates for follow-up after treatment and dataset verification. Roles in lignification, cell wall reinforcement, ROS metabolism, or stress tolerance require independent testing and cannot be concluded from these descriptive profiles.

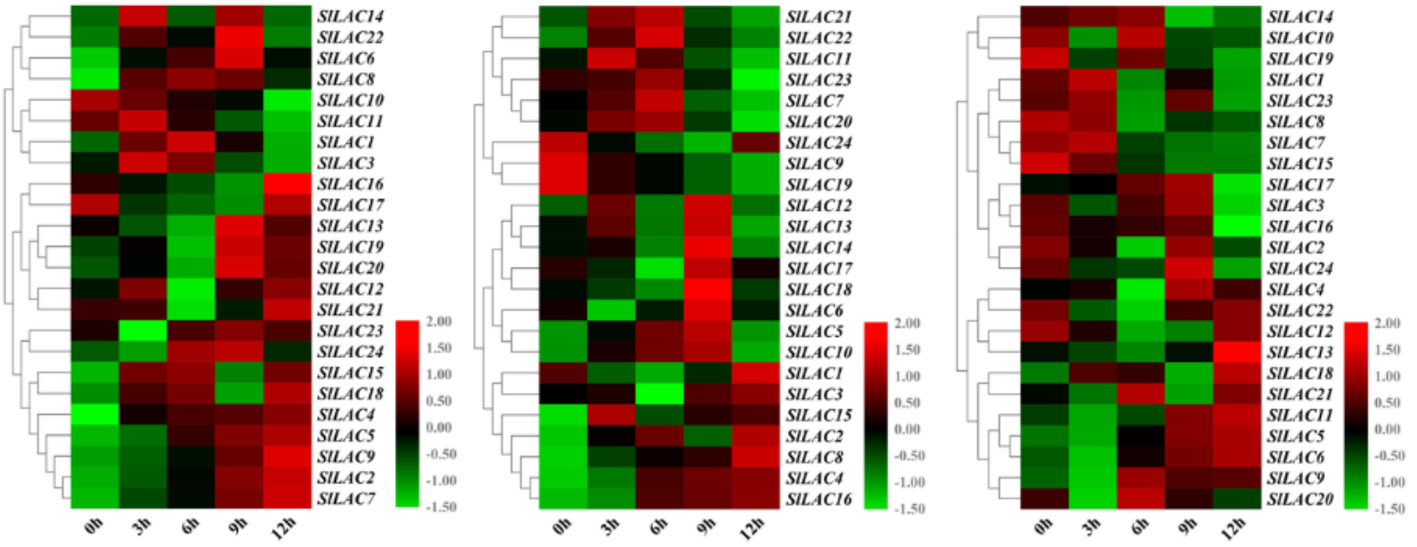


Figure 6. Reported SlLAC expression profiles for the three abiotic-stress series discussed in Results. Each panel displays 0, 3, 6, 9, and 12 h. Panel-to-treatment mapping, source data, tissue identity, normalization, color transformation, and clustering settings require confirmation. The color scale denotes plotted values, not statistical significance.

Expression Pattern Analysis of *SlLAC* Genes under Different Plant Hormone Treatments

To investigate the hormonal regulation of SlLAC genes, 12-day-old tomato seedlings were subjected to five hormonal treatments, including ethephon (Eth), gibberellic acid (GA_3), indole-3-acetic acid (IAA), salicylic acid (SA), and jasmonic acid (JA), each at a concentration of 20 µM. Samples were collected at 0, 3, 6, 9, and 12 h to evaluate temporal changes in SlLAC gene expression. Ethephon, an ethylene-releasing compound, was used to assess ethylene-associated responses. The expression profiles revealed temporal variation in SlLAC gene expression under different hormonal treatments, suggesting the potential involvement of these genes in hormone-responsive regulatory pathways (Figure 7).

In the reported Eth series, *SlLAC22*, *SlLAC11*, *SlLAC23*, and *SlLAC7* show relatively high plotted values during an early interval, whereas *SlLAC12*, *SlLAC13*, and *SlLAC18* show relatively high values later. *SlLAC16* and *SlLAC4* have lower values in parts of the displayed series (Figure 7). These patterns do not establish statistical induction or repression, or roles in fruit ripening and senescence.

The reported GA_3 series shows relatively high plotted values for *SlLAC3*, *SlLAC4*, *SlLAC10*, and *SlLAC18* at later intervals. *SlLAC12* and *SlLAC13* show different

temporal profiles (Figure 7). These observations are associations with the reported treatment and do not demonstrate effects on elongation or vascular development.

The reported IAA series shows diverse temporal profiles, including relatively high early values for *SlLAC19*, *SlLAC20*, *SlLAC10*, and *SlLAC16*, and later values for *SlLAC3*, *SlLAC7*, and *SlLAC23* (Figure 7). Visual differences among genes are not evidence of statistically significant auxin regulation or of functions in cell division and organogenesis.

The reported SA series shows diverse temporal expression patterns, including relatively high values for *SlLAC10*, *SlLAC8*, *SlLAC11*, and *SlLAC13* during intermediate intervals. *SlLAC24* and *SlLAC17* show different early and later profiles. In the reported JA series, *SlLAC3*, *SlLAC4*, *SlLAC6*, *SlLAC15*, and *SlLAC17* show relatively high values during some early intervals, while *SlLAC18*, *SlLAC19*, and *SlLAC20* show higher values later (Figure 7). These profiles do not demonstrate systemic acquired resistance, wound signaling, or direct hormone-mediated regulation.

Clustering groups genes according to the plotted hormone-series profiles. These associations are exploratory. The grouping does not demonstrate a common hormone-signaling pathway, and a statistical comparison requires replicate-level measurements and an explicitly defined analysis.

The reported hormone profiles identify candidates for subsequent expression validation and functional analysis. They do not establish causal participation in hormone signal transduction, fruit ripening, cell wall metabolism, or stress defense.

Discussion

This study reports 24 candidate tomato LAC genes with conserved multicopper-oxidase-associated sequence regions. The predicted protein lengths, molecular weights, pI values, and negative GRAVY scores describe sequence properties. Variation in these properties identifies questions for biochemical analysis, but does not establish substrate specificity, catalytic efficiency, or functional diversification. Comparative LAC-family studies provide a useful context [6, 7, 8, 9, 10, 11, 12, 32]; differences in family size cannot by themselves establish the extent or mechanism of tomato family expansion.

The chromosomal analysis places the genes on 10 of the 12 tomato chromosomes. Chromosome 5 contains five members, whereas chromosomes 6 and 9 each contain four. Variation in gene position and exon number documents structural organization, rather than demonstrated evolutionary mechanisms. No synteny, duplication classification, or Ka/Ks analysis is presented in the reported work. Consequently, tandem or segmental duplication, intron gain or loss, and selection pressures are not asserted as results. The tree descriptions have been reconciled with the supplied phylograms, and weakly supported deeper nodes limit interpretation of the relationships.

Fourteen proteins were predicted to be chloroplast-localized by WoLF PSORT, while four received extracellular assignments. Many experimentally characterized plant laccases function in extracellular or cell-wall lignification [3, 4, 33, 34]. This discrepancy is important and cannot be resolved by interpreting a localization score as an observation. The analysis did not provide signal-peptide or transit-peptide predictions, secretion experiments, or microscopy-based localization. Such work is needed to determine whether the chloroplast assignments are genuine or reflect predictor limitations. Hydrophilicity does not establish cytosolic localization and cannot resolve this discrepancy.

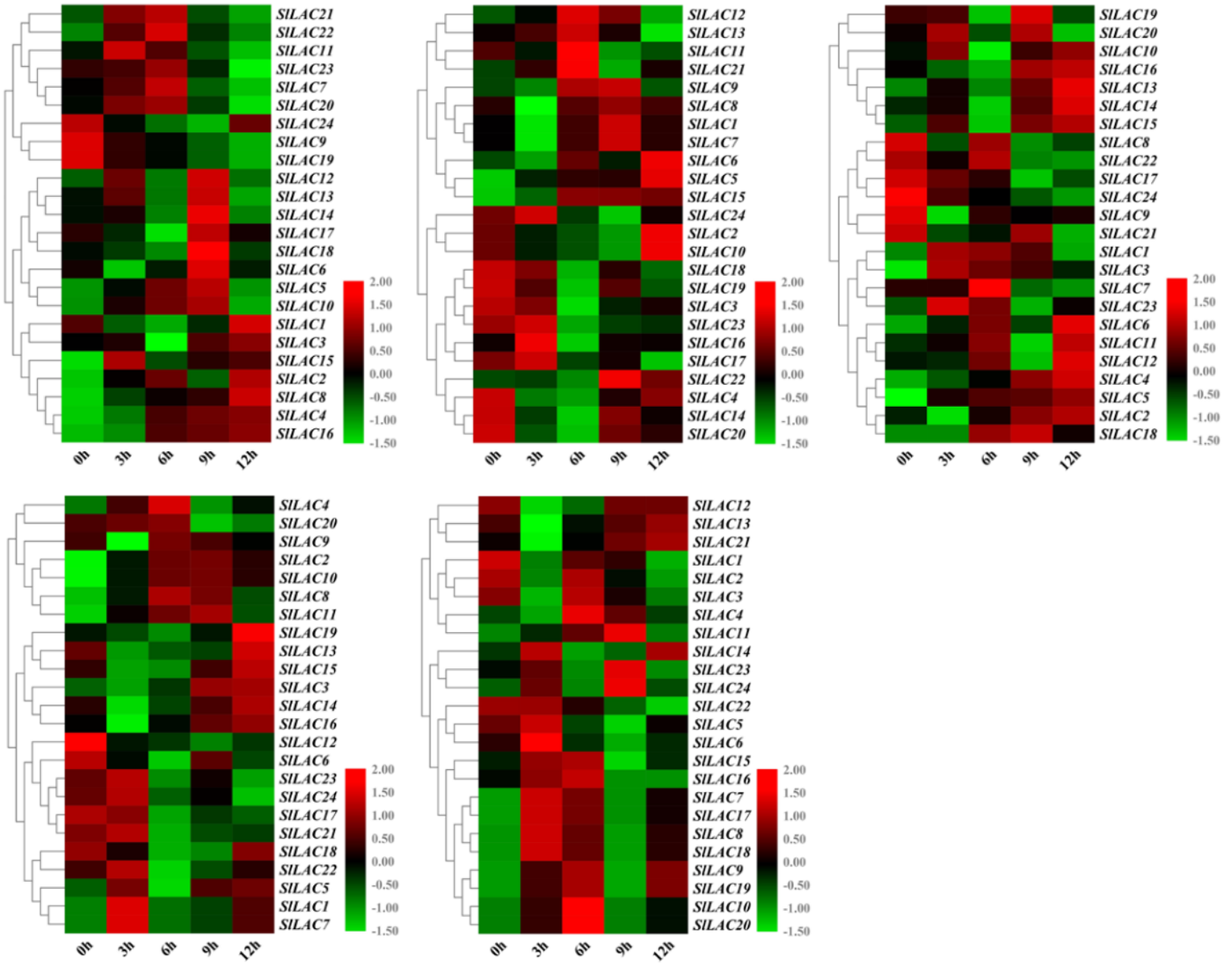


Figure 7. Reported SlLAC expression profiles for five hormonal-treatment series discussed as Eth, GA_3, IAA, SA, and JA. The displayed columns are 0, 3, 6, 9, and 12 h. Eth denotes ethephon. The panel-to-treatment mapping, sampled tissue, control normalization, color transformation, and clustering procedure require confirmation. Colors are not indicators of statistical significance.

Eight candidate genes contain predicted sly-miR397 target sites. Prior studies have demonstrated miR397-associated regulation of laccases and lignification in poplar and *Arabidopsis* [14, 15, 16]. The present psRNATarget outputs suggest testable tomato interactions, but no miR397 expression measurement, degradome analysis, cleavage assay, or genetic perturbation was reported. Expectation scores and UPE values quantify aspects of the prediction, not measured regulatory strength. No conclusion about post-stress miR397 activity in tomato is drawn.

The reported tissue, fruit-stage, stress, and hormone profiles identify candidates for follow-up. For example, the strong flower-associated profile of *SlLAC22* and the multi-tissue profile of *SlLAC23* warrant further investigation once data provenance, units, normalization, and biological replication are established. Relative expression must be interpreted

within the appropriate gene-specific control framework, rather than as absolute expression across different genes. Without replicate-based statistical analysis, visual heatmap differences cannot establish significant induction, repression, or tissue enrichment. Important reporting limitations remain. The genome assembly and ITAG release, candidate-filtering rules, and raw search outputs require documentation. Experimental sampling times are inconsistent with the figure labels, and the origins of the expression matrices are not established in the supplied text. Primer sequences, amplification efficiencies, reference-gene validation, and complete statistical reporting are needed for reproducible RT-qPCR interpretation [30]. These unresolved issues restrict the study to provisional computational and descriptive findings. Functional roles in lignification, reproductive development, hormone responses, and stress tolerance require targeted experiments, such as genetic perturbation, enzyme assays, validated localization, and confirmed miRNA-target testing.

Conclusion

The reported analysis identifies 24 candidate tomato LAC genes and describes their sequence properties, genomic organization, exploratory phylogenetic relationships, predicted localization, potential sly-miR397 targeting, and reported expression profiles. These results prioritize candidates for validation rather than establish their physiological functions. Resolving the outstanding methodological and expression-data reporting issues, followed by functional and biochemical experiments, is necessary before drawing conclusions about lignification, fruit development, hormone signaling, or stress tolerance.

Data availability

Not applicable

Acknowledgments

Not applicable

Conflict of interest

The authors declare that they have no conflict of interest.

Author Contribution

The authors confirm contribution to the paper as follows: study conception and design: SA; data collection: NA, FY; draft manuscript preparation: SA, FY; manuscript revision: SA, SB. All authors discussed the content, reviewed the results and approved the final version of the manuscript.

Funding

Not applicable

Ethics Statement

Not applicable

Publisher's note

The views expressed in this article are solely those of the authors and do not necessarily reflect those of their institutions, the publisher, editors, or reviewers. Any product mentioned is neither guaranteed nor endorsed by the publisher.

Generative AI Statement

The authors declare that generative artificial intelligence (AI) was not used in the scientific content creation, analysis, or interpretation of this manuscript. Any AI-assisted language editing or formatting support, where applicable, was carefully reviewed and verified by the authors.

Dates

Received 08 June 2026; Revised 03 November 2026; Accepted 03 November 2026; Published online 10 November 2026

References

[1] M. B. Kaczmarek, N. Kwiatos, M. Szczęsna-Antczak, and S. Bielecki, "Laccases–enzymes with an unlimited potential." Biotechnology and Food Science, vol. 81, no. 1, pp. 41-70, 2017.

[2] Y. Tobimatsu and M. Schuetz, "Lignin polymerization: how do plants manage the chemistry so well?","

Current opinion in biotechnology, vol. 56, pp. 75-81, 2019.

[3] S. Berthet, N. Demont-Caulet, B. Pollet, P. Bidzinski, L. Cézard, P. Le Bris, N. Borrega, J. Hervé, E. Blondet, S. Balzergue, C. Lapierre, and L. Jouanin, "Disruption of LACCASE4 and 17 results in tissue-specific alterations to lignification of *Arabidopsis thaliana* stems," Plant Cell, vol. 23, pp. 1124-37, 2011.

[4] Q. Zhao, J. Nakashima, F. Chen, Y. Yin, C. Fu, J. Yun, H. Shao, X. Wang, Z. Y. Wang, and R. A. Dixon, "Laccase is necessary and nonredundant with peroxidase for lignin polymerization during vascular development in *Arabidopsis*." Plant Cell, vol. 25, pp. 3976-3987, 2013.

[5] L. Pourcel, J. M. Routaboul, L. Kerhoas, M. Caboche, L. Lepiniec, and I. Debeaujon, "TRANSPARENT TESTA10 encodes a laccase-like enzyme involved in oxidative polymerization of flavonoids in *Arabidopsis* seed coat." Plant Cell, vol. 17, p. 2966–2980, 2005.

[6] J. Zhu, H. Zhang, K. Huang, R. Guo, J. Zhao, H. Xie, J. Zhu, H. Gu, H. Chen, G. Li, and C. Wei, "Comprehensive analysis of the laccase gene family in tea plant highlights its roles in development and stress responses." BMC Plant Biology, vol. 23, no. 1, p. 129, 2023.

[7] Y. Yu, Y. Xing, F. Liu, X. Zhang, X. Li, J. Zhang, and X. Sun, "The laccase gene family mediate multi-perspective trade-offs during tea plant (*Camellia sinensis*) development and defense processes," International journal of molecular sciences, vol. 22, no. 22, p. 12554, 2021.

[8] X. Ping, T. Wang, N. Lin, F. Di, Y. Li, H. Jian, H. Wang, K. Lu, J. Li, X. Xu, and L. Liu, "Genome-wide identification of the LAC gene family and its expression analysis under stress in *Brassica napus*," Molecules, vol. 24, no. 10, p. 1985, 2019.

[9] B. C. McCaig, R. B. Meagher, and J. F. Dean, "Gene structure and molecular analysis of the laccase-like multicopper oxidase (LMCO) gene family in *Arabidopsis thaliana*." Planta, vol. 221, no. 5, pp. 619-636, 2005.

[10] Q. Liu, L. Luo, X. Wang, Z. Shen, and L. Zheng, "Comprehensive analysis of rice laccase gene (OsLAC) family and ectopic expression of OsLAC10 enhances tolerance to copper stress in *Arabidopsis*." International Journal of Molecular Sciences,, vol. 18, no. 2, p. 209, 2017.

[11] Q. Wang, G. Li, K. Zheng, X. Zhu, J. Ma, D. Wang, K. Tang, X. Feng, J. Leng, H. Yu, and S. Yang, "The soybean laccase gene family: Evolution and possible roles in plant defense and stem strength selection." Genes, vol. 10, no. 9, p. 701, 2019.

[12] T. Cheng, C. Ren, J. Xu, H. Wang, B. Wen, Q. Zhao, W. Zhang, G. Yu, and Y. Zhang, "Genome-wide analysis of the common bean (*Phaseolus vulgaris*) laccase gene family and its functions in response to abiotic stress," BMC Plant Biology, vol. 24, no. 1, p. 688, 2024.

[13] X. Xu, Y. Zhou, B. Wang, L. Ding, Y. Wang, L. Luo, Y. Zhang, and W. Kong, "Genome-wide identification and characterization of laccase gene family in *Citrus sinensis*." Gene, vol. 689, pp. 114-123, 2019.

[14] S. Lu, Q. Li, H. Wei, M. J. Chang, S. Tunlaya-Anukit, H. Kim, J. Liu, J. Song, Y. H. Sun, L. Yuan, and T. F. Yeh, "Ptr-miR397a is a negative regulator of laccase genes affecting lignin content in *Populus trichocarpa*," Proceedings of the National Academy of Sciences, vol. 110, no. 26, pp. 10848-10853, 2013.

[15] C. Y. Wang, S. Zhang, Y. Yu, Y. C. Luo, Q. Liu, C. Ju, Y. C. Zhang, L. H. Qu, W. J. Lucas, X. Wang, and Y. Q. Chen, " MiR397b regulates both lignin content and seed number in *Arabidopsis* via modulating a laccase involved in lignin biosynthesis." Plant Biotechnology Journal, vol. 12, pp. 1132-1142, 2014.

[16] H. Khandal, A. P. Singh, and D. Chattopadhyay, " MicroRNA397bLACCASE2 module regulates root lignification under water- and phosphate deficiency," Plant Physiology, vol. 182, pp. 1387-1403, 2020.

[17] 100 Tomato Genome Sequencing Consortium, S. Aflitos, E. Schijlen, H. de Jong, D. de Ridder, S. Smit, R. Finkers, J. Wang, G. Zhang, N. Li, and L. Mao, "Exploring genetic variation in the tomato (*Solanum* section *Lycopersicon*) clade by whole-genome sequencing," The Plant Journal, vol. 80, no. 1, pp. 136-148, 2014.

[18] S. R. Eddy, “Accelerated profile HMM searches,” PLoS Computational Biology, vol. 7, no. 10, e1002195, 2011. doi:10.1371/journal.pcbi.1002195.

[19] I. Letunic, S. Khedkar, and P. Bork, “SMART: recent updates, new developments and status in 2020,” Nucleic Acids Research, vol. 49, no. D1, pp. D458–D460, 2021. doi:10.1093/nar/gkaa937.

[20] S. Lu et al., “CDD/SPARCLE: the conserved domain database in 2020,” Nucleic Acids Research, vol. 48, no. D1, pp. D265–D268, 2020. doi:10.1093/nar/gkz991.

[21] E. Gasteiger, C. Hoogland, A. Gattiker, S. Duvaud, M. R. Wilkins, R. D. Appel, and A. Bairoch, “Protein identification and analysis tools on the ExPASy server,” in The Proteomics Protocols Handbook, J. M. Walker, Ed. Humana Press, 2005, pp. 571–607. doi:10.1385/1-59259-890-0:571.

[22] C. Chen, Y. Wu, J. Li, X. Wang, Z. Zeng, J. Xu, Y. Liu, J. Feng, H. Chen, Y. He, and R. Xia, "TBtools-II: A “one for all, all for one” bioinformatics platform for biological big-data mining," Molecular plant, vol. 16, no. 11, pp. 1733-1742., 2023.

[23] P. Horton, K. J. Park, T. Obayashi, N. Fujita, H. Harada, C. J. Adams-Collier, and K. Nakai, "WoLF PSORT: protein localization predictor." Nucleic acids research,, vol. 35, no. (suppl_2), pp. W585-W587, 2007.

[24] B. Hu, J. Jin, A. Y. Guo, H. Zhang, J. Luo, and G. Gao, “GSDS 2.0: an upgraded gene feature visualization server,” Bioinformatics, vol. 31, no. 8, pp. 1296–1297, 2015. doi:10.1093/bioinformatics/btu817.

[25] J. D. Thompson, D. G. Higgins, and T. J. Gibson, “CLUSTAL W: improving the sensitivity of progressive multiple sequence alignment through sequence weighting, position-specific gap penalties and weight matrix choice,” Nucleic Acids Research, vol. 22, no. 22, pp. 4673–4680, 1994. doi:10.1093/nar/22.22.4673.

[26] S. Kumar, G. Stecher, and K. Tamura, “MEGA7: Molecular Evolutionary Genetics Analysis version 7.0 for bigger datasets,” Molecular Biology and Evolution, vol. 33, no. 7, pp. 1870–1874, 2016. doi:10.1093/molbev/msw054.

[27] P. Gouet, X. Robert, and E. Courcelle, “ESPript/ENDscript: extracting and rendering sequence and 3D information from atomic structures of proteins,” Nucleic Acids Research, vol. 31, no. 13, pp. 3320–3323, 2003. doi:10.1093/nar/gkg556.

[28] X. Dai, Z. Zhuang, and P. X. Zhao, “psRNATarget: a plant small RNA target analysis server (2017 release),” Nucleic Acids Research, vol. 46, no. W1, pp. W49–W54, 2018. doi:10.1093/nar/gky316.

[29] K. J. Livak and T. D. Schmittgen, “Analysis of relative gene expression data using real-time quantitative PCR and the $2^{-}\Delta\Delta CT$ method,” Methods, vol. 25, no. 4, pp. 402–408, 2001. doi:10.1006/meth.2001.1262.

[30] S. A. Bustin et al., “The MIQE guidelines: minimum information for publication of quantitative real-time PCR experiments,” Clinical Chemistry, vol. 55, no. 4, pp. 611–622, 2009. doi:10.1373/clinchem.2008.112797.

[31] P. J. Hoegger, S. Kilaru, T. Y. James, J. R. Thacker, and U. Kües, "Phylogenetic comparison and classification of laccase and related multicopper oxidase protein sequences." The FEBS journal, vol. 273, no. 10, pp. 2308-2326, 2006.

[32] P. V. Turlapati, K. W. Kim, L. B. Davin, and N. G. Lewis, "The laccase multigene family in *Arabidopsis* thaliana: towards addressing the mystery of their gene function (s)," Planta, vol. 233, no. 3, pp. 439-470, 2011.

[33] J. Wang, J. Feng, W. Jia, S. Chang, S. Li, and Y. Li, "Lignin engineering through laccase modification: A promising field for energy plant improvement," Biotechnology Biofuels, vol. 8, p. 145, 2015.[34] R. Sterjiades, J. F. Dean, G. Gamble, D. S. Himmelsbach, and K. E. L. Eriksson, "Extracellular laccases and peroxidases from sycamore maple (*Acer pseudoplatanus*) cell-suspension cultures: reactions with monolignols and lignin model compounds." Planta, vol. 190, no. 1, pp. 75-87, 1993.



Copyright: © 2026 by the author(s). Published by Inspire Science and Tech Publisher, Pakistan. This article is an open access article distributed under Creative Commons Attribution License (CC BY 4.0), visit https:// creativecommons.org/licenses/by/4.0/